Enhancement of light extraction efficiency in OLED with two-dimensional photonic crystal slabs

Rongjin Yan (闫荣金) and Qingkang Wang (王庆康)

Institute of Micro and Nano-Science and Technology, National Key Laboratory of Nano/Micro Fabrication Technology, Shanghai Jiao Tong University, Shanghai 200030

Received November 2, 2005

Light extraction efficiency of organic light emitting diode (OLED) based on various photonic crystal slab (PCS) structures was studied. By using the finite-difference time-domain (FDTD) method, we investigated the effect of several parameters, including filling factor and lattice constant, on the enhancement of light extraction efficiency of three basic PCSs, and got the most effective one. Two novel designs of "interlaced" and "double-interlaced" PCS structures based on the most effective basic PCS structure were introduced, and the "interlaced" one was proved to be even more efficient than its prototype. Large enhancement of light extraction efficiency resulted from the coupling to leaky modes in the expended light cone of a band structure, the diffraction in the space between columns, as well as the strong scattering at indium-tin-oxide/glass interfaces.

OCIS codes: 230.0230, 220.0220, 160.4670.

Four major loss mechanisms are combined to determine the efficiency of an organic light emitting diode (OLED), they are: the balance between the number of positive and negative charges injected into organic layer, the ratio of singlets to triplets in excitons, the photoluminescent quantum efficiency, and optical output coupling efficiency. The first three loss mechanisms have been widely understood and optimized[1−9], and there are also some methods introduced to improve the optical output coupling efficiency, including increasing the roughness of the top surface of glass substrate, applying lenses on the surface, reducing the thickness of indium-tin-oxide (ITO) layer, and introducing into the ITO/glass interface with aerogel or photonic crystal slabs (PCSs)[10−21]. However, the optical output coupling efficiency still remains small (0.3).

A schematic diagram of OLED structure is shown in Fig. 1(a), where only light emitted at an angle less than the critical angle can escape from the ITO/glass or glass/air interface, all other light is internally reflected back into the device. The light trapped within the device will be waveguided, eventually becoming either absorbed or emitted from the edge of the substrate, and the fraction of high index (ITO/organic) guided mode takes up almost 50% of the total energy. In this paper, we propose new design of PCS structure on the ITO/glass interface, as shown in Fig. 1(b), which could dramatically increase the efficiency of OLED.

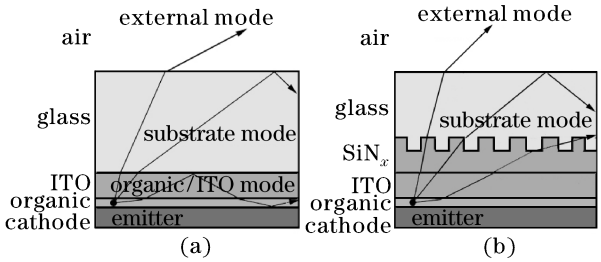

Fig. 1. (a) The light emission from a typical OLED device can be divided into three types of modes, external modes those are able to escape through the surface, and two waveguide modes which are trapped either in the substrate or in the organic/ITO layers of the device. (b) After adding PCS structure on the SiN_x layer between ITO and glass, the organic/ITO modes reduce dramatically, and thus increase the efficiency of OLED.

Optimization of the PCS is difficult, because it involves solving a multi-parameter inverse problem. There are countless combinations of lattice symmetry, scattering object shape, lattice constant, filling factor and height of PCS, but it is impossible to say which one gives the most efficient PCS structure in releasing the trapped energy in ITO/organic layer. A systematic algorithm still lacks, and the design is based on several rules of thumb. It is known that high light extraction efficiency will be gotten from the OLED based on the PCS that satisfies the following criteria: Brillouin zone is close to a circle; shape of scattering objects matches the symmetry of Brillouin zone; the lattice constant of PCS should be in the vicinity of the vacuum wavelength of the incident light. In the following, we will introduce into OLED three basic PCS structures according to these criteria, and find the most effective one for enhancing the light extraction efficiency.

Because the defects on ITO layer will result in current leakage, we introduce SiN_x layer onto ITO as a buffer layer, and deploy the PCS on it in the simulation, as shown in Fig. 1(b). Furthermore, considering the complexity of the objects, we employ the finite-difference time-domain (FDTD)[22] method for simulations.

We intercept the region on x-z-y slab as $3 \times 3 \times 4$ (μm) for calculation, put four perfect reflectors at the domain boundaries, and temporally integrate the energy extracted into the air up to the average time needed for photons to reach the surface of the unit of OLED. Meanwhile, perfectly matched layer (PML) boundary condition (0.5 μm) is put on y axis. The grid size is 0.01 μm in all the three dimensions and the time step is $\Delta t = 0.005\ \mu\text{m}/c$ with c being the velocity of light. At

the place when $y = -1.5$ μm, we put continued guided-wave as source in the organic layer and with its vacuum wavelength of 0.56 μm. Each calculation cell is setup repeatedly.

The relative light extraction efficiency E_r is defined as the ratio of light extraction efficiency of OLEDs with PCS structures E to those without PCS structures E_0.

The simulation is now targeted to examine E_r of the OLED based on the three kinds of basic PCS structures shown in Fig. 2, and find the most effective PCS design under optimized geometric parameters for further discussion. Three parameters are involved in the simulation, they are constant lattice P, height of PCS H and filling factor which is defined as $R = D_a/P$ or $R = L/P$, where D_a is the diameter of the cylinder unit cells and L is the side length of square or hexagon unit cells in different structures.

As to the PCS with square lattice of cylinder cells, we get the diagram of R versus E_r under different P, as shown in Fig. 3(a). When $P > 0.2$ μm, all values of E_r reach extrema at $R = 0.5$, namely $D_a = 0.5P$; and when $P = 0.6$ μm, E_r reaches its maximum (1.5083), which matches well with precious experimental result[18].

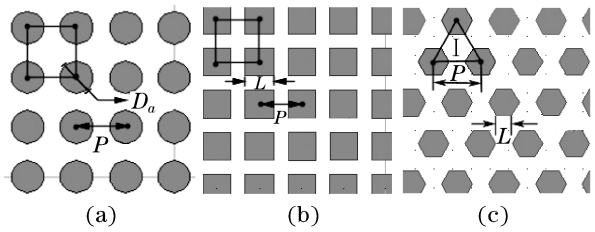

Fig. 2. PCS structures with square lattice of cylinder unit cells (a), with square lattice of square unit cells (b), and with triangular lattice of hexagon unit cells (c), introduced into the ITO/glass interface.

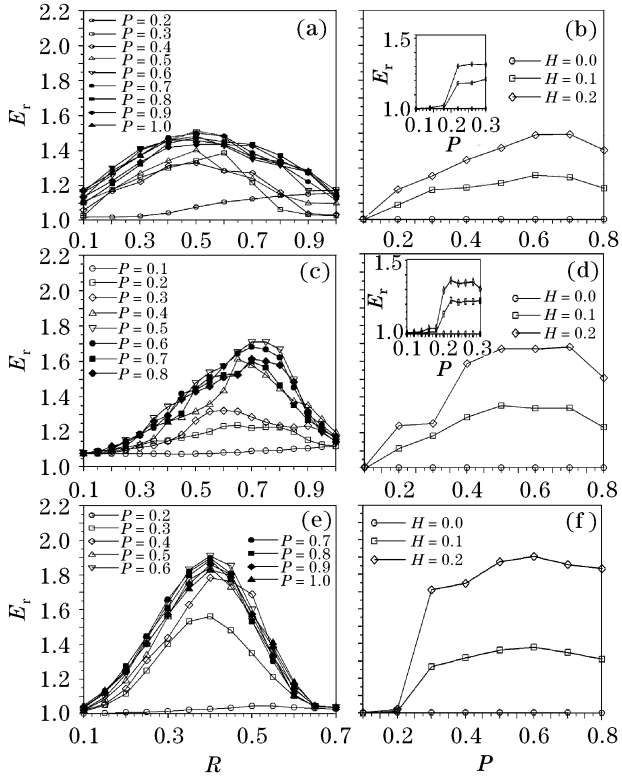

Fig. 3. Relative light extraction efficiency E_r versus filling factor R under different constant lattices P and E_r versus P under different heights of PCH H for PCSs with square lattice of cylinder unit cells (a, b), square lattice of square unit cells (c, d) and triangular lattice of hexagon unit cells (e, f).

Setting $R = 0.5$, the relationship between E_r and P could be seen more clearly in Fig. 3(b). Firstly, since we scan P from 0.1 to 0.7 μm with a relative large step of 0.1 μm, we adopt 0.04 μm as the step to further scan P from 0.1 to 0.3 μm and get the result shown in the inset of Fig. 3(b), from which we can observe the cut-off lattice constant, $P_c \approx \lambda/(n_{\text{eff}} + 1)$, where n_{eff} is the effective index of the PCS layer (~ 1.8). Below this cut-off value, leaky waves remain trapped in the glass substrate. Secondly, we can get the conclusion similar to Fig. 3(a), E_r reaches the maximum (1.5083) when $P = 0.6$ μm, which approximates vacuum wavelength of the incident light (0.56 μm). Restricted by techniques[18], we adopt two groups of height values, 0.1 and 0.2, for simulation.

For PCS with triangular lattice of hexagon unit cells, when $R > 0.7$, namely $L > 0.7P$, the layer will turn to be homogeneous medium, so we limit $R \leq 0.7$ for this PCS. As shown in Figs. 3(c) and (e), E_r of OLED, based on PCS with square lattice of square unit cells and on PCS with triangular lattice of hexagon unit cells, respectively reaches its maximum at 1.6857 when $R = 0.7$ and at 1.9112 when $R = 0.4$. Conclusions drawn from Figs. 3(d) and (f) are similar to those from Fig. 3(b).

From the above discussion, we can find that all of the three designs can enhance the light extraction efficiency of OLED dramatically, and among them, the PCS with triangular lattice of hexagon unit cells is the most effective structure with the increase of light extraction efficiency of 0.91. Thus we will introduce into ITO layer with two other new PCSs based on this basic structure to get more efficient OELD.

Firstly, we introduce another group of triangular lattice of hexagon cells into the basic PCS, as shown in Fig. 4(a). The relationships between E_r and R as well as P are shown in Figs. 5(a) and (b), from which we can see that E_r reaches its maximum at 2.0517 when $R = 0.35$ and $P = 0.6$ μm, and this proves that this "interlaced" PCS structure is more effective than the original one.

Further, we add the third group triangular lattice of hexagon cells into the structure, as shown in Fig. 4(b). Since the PCS layer turns to be homogeneous medium when $R = 3.3$, we scan R from 0.5 to 3.5 with step 0.3. The maximal value of E_r at 1.7183 when $R = 2.6$ and $P = 0.6$ μm is gotten, as shown Figs. 5(c) and (d), which means that the "double interlaced" PCS degenerates.

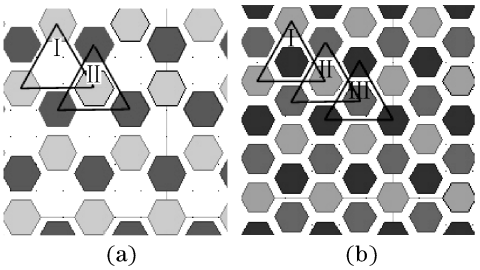

Fig. 4. PCSs with "interlaced" (a) and "double-interlaced" (b) triangular lattice of hexagon cells by introducing more triangular lattices of hexagon cells into the original structure.

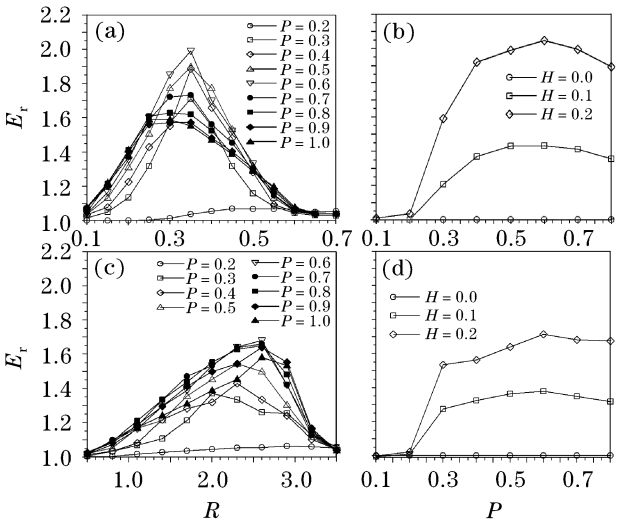

Fig. 5. Relative light-extraction-efficiency E_r versus filling factor R under different constant lattices P and E_r versus P under different heights of PCS H for PCS with "interlaced" (a, b) and "double-interlaced" triangular lattice of hexagon cells (c, d).

Now let us discuss the physical mechanism of enhancement by analyzing the energy distribution of output light in x-z plane and the band diagram of PCS. The first physical mechanism of the enhancement of the light extraction efficiency is the expanded escape cone of the internal light by a low effective refractive index of the "diluted semiconductor", namely, the average PCS medium is composed of ITO and glass which have relative small refractive index. However, the laterally directed light cannot be extracted from a simple diluted semiconductor. The second effect is that the lateral light is converted to the light toward vertical directions by the diffraction in the space between columns and the strong scattering at ITO/glass interfaces; we could observe this phenomenon in the following simulation.

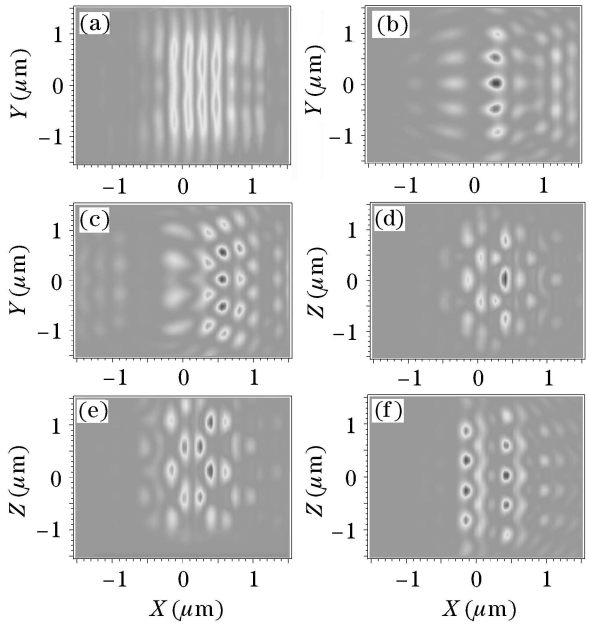

Fig. 6. Energy distribution of output light for PCS with no PCS structures (a), square lattice of cylinder unit cells (b), square lattice of square unit cells (c), triangular lattice of hexagon unit cells (d), "interlaced" triangular lattice of hexagon cells (e), and "double-interlaced" triangular lattice of hexagon cells (f).

As shown in Fig. 6, sampling at $T_c = 20\ \mu\mathrm{m}/c$, T_c is the interception time of sampling, we get the energy distribution of output light on horizontal plane (x-z plane) of OLED with five PCS structures mentioned above respectively. In the OLED without any PCS layer, the output energy is not continuously distributed along the propagation direction, since it is instantaneously sampled at T_c. Comparing Fig. 6(a) with others, we can clearly observe that after adding the PCS structure, the distribution of output light energy changes from continuous distribution which is perpendicular to the propagation direction to distribution mainly in the inter-space between columns.

As mentioned above, the different light extraction efficiencies originate partly from lower effective refractive index of the "diluted semiconductor", which could be discussed using band structures. The effective two-dimensional (2D) transverse electric (TE) band structures for three lattices (square lattice of cylinder cells, short for "square lattice"; triangular lattice of hexagon cells, short for "triangular lattice"; "interlaced" triangular lattice of hexagon cells, short for "interlaced lattice") are shown in Fig. 7. Effective refractive index used in this 2D calculation is 1.8. Dotted lines in the band structures represent the light line. Modes above the light lines

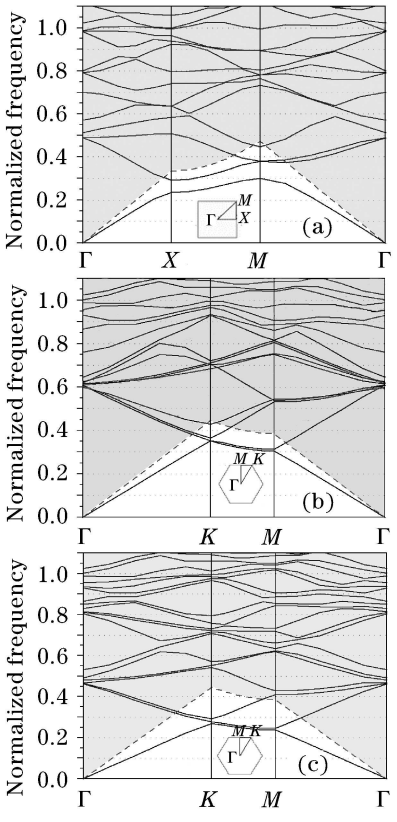

Fig. 7. 2D photonic band structure of square lattice of cylinder unit cells (a), triangular lattice of hexagon cells (b), and "interlaced" triangular lattice of hexagon cells (c) for the TE polarization. Dotted lines represent the light line above which all the modes are leaky and couple to free space.

are leaky and couple to free space (gray area)[16,23]. The bands of the triangular lattice are much denser than those of the square lattice. Note several flat bands around the normalized frequency of 1.0 in three diagrams. The normalized frequency 1.0 approximately corresponds to the lattice constant of 0.6 μm. This is the main reason for the peak enhancement with the lattice constant of 0.6 μm. In the normalized frequency larger than 0.3, the portion of guided modes is negligible in comparison with that of leaky modes and there are much more leaky modes of interlaced lattice around normalized frequency 1.0 compared with the other two lattices. This is responsible for the relatively large enhancement of interlaced lattice in comparison with the other two lattices in the lattice constant range of 0.2—0.6 μm. Therefore, the "interlaced" triangular lattice of hexagon cells shown in Fig. 4(a) might be the best one in the three kinds of lattices.

We introduce into ITO layer with three basic designs of PCS, all of which follow the design criteria, and by comparing $E_{\rm r}$ of OLED based on these three PCS structures, we find that the filling factor has important impact on $E_{\rm r}$, and the value corresponding to the maximal $E_{\rm r}$ changes from 0.4 to 0.75 along with the variety of unit cell shape; under optimized filling factors, $E_{\rm r}$ reaches its maximum when lattice constant equates 0.6 μm, which approximates the vacuum wavelength of the incident light. We get the most effective basic design, the PCS with triangular lattice of hexagon unit cells, and, further, we introduce other groups of the same PCS into it to form the "interlaced" and "double-interlaced" PCSs with triangular lattice of hexagon unit cells, and the so-called "interlaced" PCS is proved to be even more effective than the original design in enhancing $E_{\rm r}$ of OLED. By examining the energy distribution of output light in horizontal plane and the band structure of two typical PCS structures, we discuss two physical mechanisms of the enhancement. Discussions about the design process, impact of parameters of PCS as well as physical mechanisms provide new ideas to further improve the performance of OLED and other areas related to the transmission-enhancement or anti-reflection in visible spectrum.

This work was supported by the 2005 Nano-Science and Technology Foundation of Science and Technology Committee of Shanghai Municipality under Grant No. 0452nm056. Q. Wang is the author to whom the correspondence should be addressed, his e-mail address is wangqingkang@sjtu.edu.cn.

References

1. G. G. Malliaras and J. C. Scott, J. Appl. Phys. **85,** 7426 (1999).
2. B. K. Crone, I. H. Campbell, P. S. Davids, D. L. Smith, C. J. Neef, and J. P. Ferraris, J. Appl. Phys. **86,** 5767 (1999).
3. D. F. O'Brien, M. A. Baldo, M. E. Thompson, and S. R. Forrest, Appl. Phys. Lett. **74,** 442 (1999).
4. B. Chen, Y. Liu, C. S. Lee, G. Yu, S. T. Lee, H. Li, W. A. Gambling, D. Zhu, H. Tian, and W. Zhu, Thin Solid Films **363,** 173 (2000).
5. Y. Kawabe, G. E. Jabbour, S. E. Shaheen, B. Kippelen, and N. Peyghambarian, Appl. Phys. Lett. **71,** 1290 (1997).
6. M. A. Baldo, D. F. O'Brien, Y. You, A. Shoustikov, S. Sibley, M. E. Thompson, and S. R. Forrest, Nature **395,** 151 (1998).
7. P. W. M. Blom, M. C. J. M. Vissenberg, J. N. Huiberts, H. C. F. Martens, and H. F. M. Schoo, Appl. Phys. Lett. **77,** 2057 (2000).
8. R. W. T. Higgins, A. P. Monkman, H.-G. Nothofer, and U. Scherf, J. Appl. Phys. **91,** 99 (2002).
9. H. Becker, S. E. Burns, and R. H. Friend, Phys. Rev. B **56,** 1893 (1997).
10. T. Tsutsui, N. Takada, S. Saito, and E. Ogino, Appl. Phys. Lett. **65,** 1868 (1994).
11. A. Dodabalapur, L. J. Rothberg, T. M. Miller, and E. W. Kwock, Appl. Phys. Lett. **64,** 2486 (1994).
12. R. Windisch, P. Heremans, A. Knobloch, P. Kiesel, G. H. Döhler, B. Dutta, and G. Borghs, Appl. Phys. Lett. **74,** 2256 (1999).
13. G. Gu, D. Z. Garbuzov, P. E. Burrows, S. Venkatesh, S. R. Forrest, and M. E. Thompson, Opt. Lett. **22,** 396 (1997).
14. C. F. Madigan, M.-H. Lu, and J. C. Sturm, Appl. Phys. Lett. **76,** 1650 (2000).
15. T. Tsutsui, M. Yahiro, H. Yokogawa, K. Kawano, and M. Yokoyama, Adv. Mater. **13,** 1149 (2001).
16. S. Fan, P. R. Villeneuve, J. D. Joannopoulos, and E. F. Schubert, Phys. Rev. Lett. **78,** 3294 (1997).
17. M. Boroditsky, T. F. Krauss, R. Coccioli, R. Vrijen, R. Bhat, and E. Yablonovitch, Appl. Phys. Lett. **75,** 1036 (1999).
18. Y.-J. Lee, S.-H. Kim, J. Huh, G.-H. Kim, Y.-H. Lee, S.-H. Cho, Y.-C. Kim, and Y. R. Do, Appl. Phys. Lett. **82,** 3779 (2003).
19. H.-Y. Ryu, J.-K. Hwang, Y.-J. Lee, and Y.-H. Lee, IEEE J. Sel. Top. Quantum Electron. **8,** 231 (2002).
20. J. Song, Y. Fu, Y. Liu, Y. Chang, B. Kang, X. Li, and G. Du, Semiconductor Optoelectronics (in Chinese) **21,** 214 (2000).
21. M. Kitamura, S. Iwamoto, and Y. Arrakawa, Jpn. J. Appl. Phys. **44,** 2844 (2005).
22. K. Yee, IEEE Trans. Antennas Propagat. **14,** 302 (1966).
23. O. Painter, J. Vuckovic, and A. Scherer, J. Opt. Soc. Am. B **16,** 276 (1999).